PPPL--2390

DE87 003074

EXPERIMENTAL RESULTS FROM THE TFTR TOKAMAK

R.J. Hawryluk, V. Arunasalam, J.D. Bell[a], M.G. Bell, M. Bitter, W.R. Blanchard, F. Boody, N. Bretz, R. Budny, C.E. Bush[a], J.D. Callen[c], J.L. Cecchi, S. Cohen, R.J. Colchin[a], S.K. Combs[a], J. Coonrod, S.L. Davis, D. Dimock, H.F. Dylla, F.C. Elthimion, L.C. Emerson[a], A.C. England[a], H.P. Eubank, R. Fonck, E. Fredrickson, L.R. Grisham, R.J. Goldston, B. Grek, R. Groebner[d], H. Hendel[e], K.W. Hill, D.L. Hillis[a], E. Hinnov S. Hiroe[a], R. Hulse, H. Hsuan, D. Johnson, L.C. Johnson, R. Kaita, R. Kamperschroer, S.M. Kaye, S. Kilpatrick, H. Kugel, P.H. LaMarche, R. Little, C.H. Ma[a], D.M. Manos, D. Mansfield, M. McCarthy, R.T. McCann, D.C. McCune, K. McGuire, D.M. Meade, S.S. Medley, S.L. Milora[a], D.R. Mikkelsen, W. Morris[f], D. Mueller, M. Murakami[a], E. Nieschmidt[g], D.K. Owens, V.K. Pare[a], H. Park, B. Prichard, A. Ramsey, D.A. Rasmussen[a], M.H. Redi, A.L. Roquemore, N.R. Sauthoff, J. Schivell, G.L. Schmidt, S.D. Scott, S. Sesnic, M. Shimada[h], J.E. Simpkins[a], J. Sinnis, F. Stauffer[b], B. Stratton, G.D. Tait, G. Taylor, C.E. Thomas[a], H.H. Towner, M. Ulrickson, S. von Goeler, R. Wieland, J.B. Wilgen[a], M. Williams, K.L. Wong, S. Yoshikawa, K.M. Young, M.C. Zarnstorff, and S. Zweben

Plasma Physics Laboratory, Princeton University

P.O. Box 451, Princeton, NJ 08544

[a]Permanent address: Oak Ridge National Laboratory, Oak Ridge, TN

[b]Permanent address: University of Maryland, College Park, MD

[c]Permanent address: University of Wisconsin, Madison, WI

[d]Permanent address: GA Technologies, Inc., San Diego, CA

[e]Permanent address: RCA David Sarnoff Research Center, Princeton, NJ

[f]Permanent address: Balliol College, University of Oxford, UK

[g]Permanent address: EG&G, Idaho

[h]Permanent address: Japan Atomic Energy Research Institute, Japan

Abstract

Recent experiments on TFTR have extended the operating regime of TFTR in both ohmic- and neutral-beam-heated discharges. The TFTR tokamak has reached its original machine design specifications (I_p = 2.5 MA and B_T = 5.2 T). Initial neutral-beam-heating experiments used up to 6.3 MW of deuterium beams. With the recent installation of two additional beamlines, the power has been increased up to 11 MW. A deuterium pellet injector was used to increase the central density to 2.5 x 10^{20} m^{-3} in high current discharges. At the opposite extreme, by operating at low plasma current (I_p ~ 0.8 MA) and low density ($\bar{n}_e$ ~ 1 x 10^{19} m^{-3}), high ion temperatures (9 ± 2 keV) and rotation speeds (7 x 10^5 m/s) have been achieved during injection. In addition, plasma compression experiments have demonstrated acceleration of beam ions from 82 keV to 150 keV, in accord with expectations. The wide operating range of TFTR, together with an extensive set of diagnostics and a flexible control system, has facilitated transport and scaling studies of both ohmic- and neutral-beam-heated discharges. The results of these confinement studies are presented.

I. Introduction

The goals of the TFTR device are (1) to study reactor-grade plasmas with temperatures ~ 10 keV and densities ~ 10^{20} m^{-3}, and (2) to achieve approximate energy breakeven between the power input to and the fusion output from the plasma (Q ~ 1). These objectives require the application of intense neutral beam heating with a full energy of 120 keV, and eventually tritium target plasmas. The increasingly wide operating range of TFTR has facilitated transport and scaling studies in both ohmic- and neutral-beam-heated discharges. With the installation of two additional beamlines, for a total of

four, the neutral beam power has been increased up to ~ 11 MW and in the course of a year will approach its design goal of 27 MW. The focus of the next series of experiments will be to optimize the plasma performance at these higher power levels in preparation for a demonstration in 1987 of $Q \sim 1$ equivalent conditions in deuterium discharges.

Two principal approaches exist for demonstrating $Q \sim 1$ in TFTR. The first is in the standard neutral-beam-heating regime ($\bar{n}_e \gtrsim 5 \times 10^{19}$ m^{-3} where $\bar{n}_e$ is the line-averaged density) at full power. In this regime, beam-target and thermonuclear reactions predominate. Achieving $Q \sim 1$, in this regime, will require energy confinement times of ~ 300 ms at full heating power (Eubank et al. 1985). The second is the energetic ion regime in which beam-beam and beam-target reactions dominate. This is a low-density regime in which the energy stored in the fast ions is relatively large and the $n_e\tau_E$ required to achieve $Q \sim 1$ can be reduced significantly (Jassby 1976). Yet another alternative is to supplement neutral beam heating with adiabatic compression by rapidly reducing the major radius. Adiabatic compression not only increases the plasma density and temperature but also increases the fast-ion energy and thus the plasma reactivity.

In this paper, a brief description of the device and the present status will be given. The operating region for ohmic- and neutral-beam-heated discharges will be described, followed by a description of parametric scaling studies of ohmically heated discharges. Neutral-beam-heating scaling and profile studies in the standard regime ($\bar{n}_e \gtrsim 3 \times 10^{19}$ m^{-3} for $P_{inj} \lesssim 11$ MW) will be discussed. A brief review of adiabatic compression results will be given, followed by a discussion of novel observations in the energetic ion regime.

II. Machine Status

TFTR is a circular tokamak with an air-core transformer. The resistance of the vacuum vessel is relatively high (3.1 mΩ) to accommodate major-radius compression experiments. A flexible control and power supply system facilitates exploration of a wide range of different operating regimes. Feedback systems are used to control the plasma current, major radius, vertical displacement, and electron density (Hawryluk et al. 1984 and Mueller et al. 1986). A description of the diagnostics is given by Johnson and Young (1983).

An initial series of experiments with two neutral beamlines was completed in April 1985 during which time TFTR reached its original machine design specifications in plasma current and toroidal field (I_p = 2.5 MA and B_T = 5.2 T). Subsequently, major upgrades to the neutral-beam-heating system and vacuum vessel components have taken place.

The neutral beam injection system was composed of two beamlines operating at ~ 80 kV, both injecting tangentially in the direction of the plasma current (co-injection). The maximum power, using deuterium beams, was 6.3 MW with a pulse duration of 0.5 s. Subsequently, two additional beamlines were installed. Of these, one beamline is in the direction of the plasma current and one opposite (counter-injection). A summary of the neutral beam system parameters is given in Table 1. The tangency radii of the different beam sources were chosen to vary from 1.74 to 2.84 m to facilitate neutral beam power deposition profile studies. At a fixed plasma position, it is possible to select beams to preferentially heat the plasma core or the plasma edge. This capability will facilitate detailed studies to test various transport models as discussed below. At the end of 1986, the beam system will be modified to provide higher average energy particles and longer pulse duration as shown in Table 1.

Prior to April 1985, the major internal vacuum vessel components were the moveable limiter assembly, bellows cover plates, and a partial set of protective plates to guard against damage of the vacuum vessel wall due to neutral beam power deposition. During that run, the plasma was principally limited by the moveable limiter assembly composed of three water-cooled Inconel blades covered with graphite tiles. For the large plasma experiments, the plasma major radius, R, was typically 2.58 m and the plasma minor radius, a, was 0.82 m. During the recent installation period, the inner wall Inconel bellows cover plates were replaced with an axisymmetric inner wall bumper limiter. This limiter is composed of water-cooled Inconel plates covered with graphite tiles, and is able to handle much more power than the moveable limiter. The inner wall limiter defines the present large plasma dimensions to R = 2.48 m and a = 0.82 m. The full complement of protective plates was also installed.

Towards the end of the initial set of experiments with two neutral beams, a repeating pneumatic pellet injector developed at Oak Ridge National Laboratory (Combs et al. 1985) was installed and successfully operated to fuel the discharge. The injector was operated in deuterium to produce single 4 mm diameter (2.1×10^{21} D°) pellets at 1300 m/s, or multiple 2.67 mm diameter (7×10^{20} D°) pellets at up to 1350 m/s. The injector is capable of producing 4 mm pellets at 1900 m/s when operated in hydrogen. In May 1986, a more flexible eight-barrel pneumatic injector will be installed with different size pellets to optimize the fueling deposition profile and hence the density profile.

III. Operating Range

The operating range for large plasmas during the two neutral beam experiments conducted on the moveable limiter is illustrated by means of the Hugill diagram shown in Fig. 1 where q_a is the limiter safety factor. The approach to the high density limit is characterized by the occurrence of high edge radiation, which begins near the inner wall as a MARFE (Lipschultz et al. 1984), and finally by high density disruptions. In deuterium gas-fueled discharges, the density limit corresponds to a Murakami parameter $\bar{n}_e$ R/B_t, of ~ 3.2 x 10^{19} m^{-2} T^{-1}. By means of pellet injection or the use of helium as the working gas, higher line-averaged densities of up to 8 x 10^{19} m^{-3}, corresponding to a Murakami parameter of ~ 5.6 x 10^{19} m^{-2} T^{-1}, were achieved during operation on the moveable limiter (Schmidt et al. 1985). Recent pellet injection experiments on the inner wall have produced Murakami values of 6.5 x 10^{19} m^{-2} T^{-1} and a line-averaged density of 1.4 x 10^{20} m^{-3}. Near the gas-fueled density limit, by carefully programming the current and density waveforms, it is possible to establish stable discharges with a cold radiating mantle surrounding the plasma that isolates the hot core from contact with the limiter for many energy confinement times (Strachan et al. 1985). The stability of these discharges and the observation that the density limit is different for gas-fueled and pellet-fueled discharges suggests that the density limit is not merely defined by thermal stability due to the temperature dependence of impurity radiation as analyzed previously by Gibson (1976), Rebut and Greene (1977), Ashby and Hughes (1981), Ohyabu (1979), Roberts (1983), and Perkins and Hulse (1985), but is also affected by the fueling profile and plasma recycling.

The low density limit is determined by recycling from the limiter and the particle confinement time. With increasing plasma current, the low density

limit increases. Thus, in order to obtain the low density discharges, of particular importance in the energetic ion regime studies, reduced current operation has been required.

In ohmically heated discharges, Z_{eff} decreases with increasing density. According to visible bremsstrahlung and x-ray pulse-height-analysis measurements and neoclassical resistivity calculations, $Z_{eff} = 1.2$ has been achieved in high density discharges defined by either the moveable limiter or the inner bumper limiter. During a neutral beam power scan at an intermediate density of $\simeq 4.6 \times 10^{19}$ m^{-3} on the moveable limiter, Z_{eff} was found to increase from $\simeq 1.8$ to $\simeq 2.8$ with increasing power up to an injected power of 5.6 MW. Recent experiments on the inner graphite bumper limiter do not show a significant increase in Z_{eff} up to an injected power of $\simeq 11$ MW (with $Z_{eff} \lesssim 2$) as determined by pulse-height-analysis measurements and neoclassical resistivity calculations. The principal impurity is carbon which determines both Z_{eff} and the dilution of deuterium ions, though oxygen impurities appear to play an important role at the density limit (Dylla et al. 1986).

In typical high current discharges, the most prominent type of MHD activity is sawtooth oscillations (McGuire et al. 1985). Sawteeth appear to play an important role in determining the temperature profile shape in the core of the discharge. However, they have little effect on the overall energy balance under present operating conditions (Murakami et al. 1985b).

IV. Confinement in Ohmically Heated Discharges

Previous experiments (Hawryluk et al. 1984, Efthimion et al. 1985) at modest toroidal fields ($\lesssim 2.8$ T) and plasma currents ($\lesssim 1.4$ MA) demonstrated that the global energy confinement time, τ_E, scales as $\bar{n}_e q_a R^2 a$ reaching a maximum value of $\tau_E \sim 0.3$ s. Recent ohmic experiments utilizing both gas- and

pellet-fueled discharges have concentrated on exploring the applicability of the previous scaling law over a wider operating range in density, toroidal field, and plasma current.

The analysis of the energy confinement time has relied upon the time-independent kinetic analysis code, SNAP. Figure 2 is a summary of the ohmic-heating studies for large plasmas on the moveable limiter. In gas-fueled deuterium discharges, the confinement time increases up to 0.44 s, in reasonable agreement with $n_e q_a$ scaling for $\bar{n}_e \lesssim 4.8 \times 10^{19}$ m^{-3}. However, in both high density helium discharges as well as high density deuterium pellet discharges, the confinement time no longer increases linearly with line-averaged density. The rollover in the density scaling of ohmically heated discharges is in fair agreement with the predictions of the empirical confinement model proposed by Goldston (1984), assuming that the H-mode scaling applies in these ohmic discharges. [This corresponds to multiplying the L-mode auxiliary confinement time by a factor of two.] L-mode scaling significantly underestimates both the confinement time and the density at which the transition from linear density scaling occurs. In the high density regime, the confinement time is observed to be only a weak function of plasma current, also in fair agreement with Goldston's H-mode model. Analyses of the energy balance for helium discharges in the high density regime, utilizing Thomson scattering electron temperature profile measurements and Doppler broadening measurements of the TiXXI K_α line to determine the central ion temperature, indicate that the electron channel and not the ion channel is responsible for the rollover, assuming that electron-ion heat transfer is due to Coulomb collisions. However, small systematic errors in either measurement could alter this conclusion since $(T_e - T_i)/T_e \ll 1$ so that, at present, it is not possible to exclude the possibility that ion transport is responsible for

the rollover as indicated in the Alcator-C experiments (Greenwald et al. 1985).

In addition to increasing the line-averaged density, pellet injection enables the formation of highly peaked density profiles. A line-averaged density of 1.4×10^{20} m^{-3} has been achieved following the injection of three 2.7 mm pellets in recent experiments conducted on the inner graphite limiter. The central electron density was 2.5×10^{20} m^{-3} and the central electron temperature was 1.25 keV as measured by Thomson scattering 400 ms after the last pellet was injected. The line-averaged density decreased to 1.1×10^{20} m^{-3} by this time. The energy confinement time was ~ 0.40 s according to kinetic and diamagnetic measurements corresponding to an $n_e(0)\, \tau_E \simeq 1 \times 10^{20}$ m^{-3} s. The radiation loss on axis in these high density discharges due to bremsstrahlung collisions (Karzas and Latter 1961), p_b, is $\simeq$ 50 kW/m^3 for a pure hydrogenic plasma. This is a significant fraction of the local ohmic input power, $p_b/p_{OH} \sim 0.2$, unlike in typical tokamak discharges. That bremsstrahlung may be important has been previously recognized. Pease (1957) pointed out the general constraints imposed on pinches when bremsstrahlung radiation equals the ohmic input power.

This peaked density profile was achieved by decreasing the plasma minor radius to 0.7 m and the plasma current to 1.6 MA in order to improve the pellet penetration. For a given pellet size and speed, an optimum target plasma needs to be established for adequate penetration because of the strong dependence of the ablation rate of the pellet on electron temperature. The new eight-barrel pneumatic injector with multiple pellet size and independent firing time will provide additional flexibility to optimize the deposition profile further.

V. Neutral-Beam-Scaling Studies

The variation of energy confinement time with injection power up to ~ 11 MW was systematically studied by operating so that the density at the end of the injection pulse was approximately constant ($\bar{n}_e$ = 4.2-4.8 x 10^{19} m^{-3}). These experiments were conducted in the large plasma configuration on the inner wall limiter with deuterium gas fueling, deuterium beams, I_p = 2.2 MA, and B_T = 4.8 T. Because there was a large power-dependent density rise due to the beam ($\Delta\bar{n}_e/\bar{n}_e$ up to ~ 0.7 at P_{inj} ~ 11 MW), the density before injection was decreased as the power increased to maintain the approximately constant final density. In this power scan, the electron and ion temperature in ohmically heated discharges was ~ 2.5 keV. At P_{inj} = 10 MW, the electron temperature increased to ~ 4 keV according to Thomson scattering and x-ray pulse-height-analysis measurements, while the ion temperature increased to ~ 5.2 keV according to FeXXV K_α Doppler-broadening measurements. Measurements of the neutron flux using the techniques described by Hendel (1986) show that the neutron source strength increases with injected power up to ~ 1 x 10^{15} n/s. The calculated neutron source strength using the K_α Doppler-broadening measurements for the central ion temperature and assuming classical slowing down of the fast ions in gas-fueled neutral-beam-heated discharges is typically a factor of ~ 2 larger than the measured neutron source strength. A similar discrepancy was also observed in the compression experiments (Wong et al. 1985) and in gas-fueled ohmic experiments. The reasons for the discrepancy are under investigation.

Figure 3 shows the variation in the total stored energy in the thermal ions (W_i), electrons (W_e), and beam ions (W_b) with heating power (P_{heat}) for the 2.2 MA power scan. Both kinetic and diamagnetic loop measurements are shown. Because the energy stored in the beam ions is evaluated to be small,

the interpretation of the diamagnetic measurements assumed the plasma was isotropic. The heating power (P_{heat}) is defined as the sum of the ohmic (P_{OH}) and the absorbed beam power (P_{abs}) after subtraction of the calculated fast-ion charge exchange loss (P_{cx}), which is 8-15% of P_{abs} in these experiments. The stored energy increases linearly with heating power; however, the rate of increase of stored energy, dW_p/dP_{heat}, is appreciably less than the ohmic confinement time. The less-than-expected increase in stored energy is due to degradation of the global energy confinement with auxiliary heating. Previous measurements of the power radiated and the heat flux to the limiter in the standard neutral-beam-heating regime are in good agreement (within ± 10%) with the ohmic- and neutral-beam-heating power (Murakami et al. 1985a).

The gross energy confinement time $\tau_E(a)$ ($\equiv W_p/P_{heat}$ in equilibrium where $W_p = W_e + W_i$) for the data shown in Fig. 3 fits the form of $\alpha + \beta/P_{heat}$ where the "incremental" confinement time $\alpha = 0.09$ s for 2.2 MA discharges. An alternative and commonly used technique is to fit $\tau_E(a)$ by a power law dependence of $P^{-\gamma}_{heat}$ where $\gamma = 0.6$ for this data. For high current TFTR discharges, both formulations result in similar extrapolations for $\tau_E(a)$ for when the heating power will be increased to 27 MW. Figure 4 shows the variation of $\tau_E(a)$ with power and the predictions of the empirical scaling model proposed by Goldston (1984). As mentioned above, the ohmic results are in fair agreement with the H-mode model; however, the high power beam-heating results are in better accord with the L-mode model. These recent results are in good agreement with the previous results reported by Murakami et al. (1985b) on experiments conducted on the moveable limiter at the same plasma current and density. In those experiments with $P_b \leq 5.6$ MW, the energy confinement time was typically 10-15% greater at the same power. Figure 5 shows the favorable variation of $\tau_E(a)$ with plasma current as found in smaller

tokamaks with injection (Murakami et al. 1985b). In TFTR, variations in plasma current are typically accompanied by variations in electron density. A joint confidence analysis of the database for auxiliary heating indicates that $\tau_E(a)$ is indeed a strong function of plasma current and a weak function of density.

The degradation of confinement time with power was anticipated based on the performance of smaller tokamaks. On smaller devices, a variety of techniques has been effective in increasing the confinement time (see references in the review paper by Kaye, 1985). The most successful technique has been the use of a divertor to define the plasma boundary (Keilhacker et al. 1985, Kitsunezaki et al. 1985, Fonck et al. 1984, and Overskei et al. 1984). In limited discharges, by carefully admitting low-Z impurities (Lazarus et al. 1984), by injecting pellets (Sengoku et al. 1985), or by the use of a pumped limiter on the large major-radius side (Budny et al. 1984), enhancements in the energy confinement time have been achieved. In the upcoming series of experiments, the goal will be to extend techniques which have worked successfully on smaller devices and to develop new ones suitable for the present larger higher power tokamaks such as JET, TFTR, and JT-60. Though the empirical scaling models provide a useful benchmark for evaluating the efficiency of confinement enhancement techniques and device performance, the reasonable agreement between the empirical scaling models and the experimental results is not an indication of a fundamental understanding of plasma transport. This is shown by the results on smaller devices which exceeded the predictions of L-mode scaling. Indeed reproducing these enhanced confinement results on a larger machine would be a major step towards enhancing this understanding.

VI. Profile Variations During Neutral Beam Injection

The heating profile during neutral beam injection is primarily determined by the beam energy distribution, injection angle, beam species, and plasma density profile. In comparison with the ohmic heating profiles, which during the current flattop are peaked on axis, the beam-heating profiles, especially with D° beams and high density discharges, can be much broader and in some cases even hollow. Thus, one might expect that the shape of the temperature profile would be substantially different during neutral beam injection. However, this is not observed.

In TFTR ohmic studies, Taylor et al. (1985) have shown that the electron temperature profiles are correlated with q_a. Similarly, in PDX neutral-beam-heating studies, Goldston (1984) and Kaye et al.(1984) demonstrated that the ratio $\langle T_e \rangle / T_e(0)$, where $\langle T_e \rangle$ is the volume-averaged T_e, is a function of $1/q_a$ independent of beam power. Figure 6 shows the sawtooth-averaged $\langle T_e \rangle / T_e(0)$ as a function of $1/q_a$ for TFTR discharges (Murakami et al. 1985b). In addition, the radius of the $q = 1$ surface (as determined by the soft x-ray imaging system) is also observed to be a function of $1/q_a$ for the same data independent of beam power (Murakami et al. 1985b). These studies were conducted during the flattop phase of the plasma current pulse in order to minimize variations in the current density profile associated with the current penetration phase and the development of the $q = 1$ surface. That both $\langle T_e \rangle / T_e(0)$ and the radius of the $q = 1$ surface are functions of $1/q_a$ suggests that there are natural profile shapes for $T_e(r)$ and possibly $q(r)$ associated with the limiter safety factor. Coppi (1980), Perkins (1984), and others have discussed the implications of a constrained temperature profile for anomalous transport. Recently, Furth (1985) and Furth et al. (1985) have discussed the constraints on current profile shape imposed by resistive kink stability requirements and their ramifications.

At present, further experiments are in progress to examine whether the current or the temperature profile is more severely constrained by q_a. In equilibrium, the current and temperature profile are related by the plasma conductivity. By applying a strong current ramp of up to 2.8 MA/s (starting at I_p = 1.4 MA and increasing to 2.2 MA), the current and temperature profiles have been transiently perturbed. Despite the large current ramp-up rate, the current penetration can be successfully modelled using a one-dimensional magnetic field diffusion code, TRANSP (Hawryluk 1980), using the measured electron temperature profile and assuming neoclassical resistivity. Bursts of MHD activity, which occur at the highest ramp rate (typically when q_ψ is ~ 4), result in a significant decrease of the electron temperature in the plasma periphery which has been taken into account in the analysis. Detailed analysis of these discharges during beam injection experiments is in progress.

That the electron temperature profile shape (with electric field approximately constant across the profile) is a weak function of beam power and is similar to the ohmic temperature profile has several interesting implications since the heating profile in beam-heated discharges is different from the ohmic heating profile. Murakami et al. (1985a) showed that, despite shallow beam penetration with D° injection, $\tau_E(a)$ values are as large as those with more penetrating H° injection, and that the central core confinement is greater with D° injection. Similar results have been reported by Speth et al. (1985) on neutral beam experiments conducted in ASDEX. These observations are similar to the T-10 electron-cyclotron-heating results which showed that the confinement time remained roughly constant as the resonance layer was moved from r = 0 to r ~ 0.5 a (Alikaev et al. 1985). Figure 7 shows the fraction of the plasma stored energy, F_W, within r = a/3 as a function of the fraction of the heating power, F_p, deposited within r = a/3. In ohmic discharges, F_W

increases as F_p is raised by raising q_a. With neutral beam injection, F_p varies over a much wider range (a factor of 5); however, the variation in F_W is no broader than in the ohmic case and is determined basically by q_a rather than by F_p. Since $F_W/F_p = \tau_E(a/3)/\tau_E(a)$, this indicates that the core confinement with poorly penetrating beams (in particular with pellet-fueled beam-heated plasmas) is substantially greater than the gross energy confinement.

Schmidt et al. (1985), using a time-dependent kinetic analysis code, TRANSP (Hawryluk 1980, and Goldston et al. 1984), has shown that in the pellet-fueled discharges the central energy confinement time $\tau_E(a/3)$ is ~ 1 s; however, the global energy confinement is ≈ 0.2 s which is similar to that in lower density gas-fueled discharges. The results of the analysis indicate that the improvement in the central confinement time is due to a reduction in the thermal diffusivity and not due to a reduction in the thermal gradients (i.e., the temperature profile is largely consistent). Furth (1985) and Zweben, Redi, and Bateman (1986) have pointed out that the high density, non-centrally heated regime which can be achieved with pellet injection should lend itself to the study of alpha-heating effects. Under these conditions, the central region is expected to have a favorable $n\tau_E$ value, along with minimal levels of nonfusion background power deposition.

In these experiments the large variations in heating profile were accompanied by variations in electron density. Thus while the global energy confinement was not found to vary with density, part of the variation in the central confinement time may be due to a change in the central density. Experiments are in progress to examine this by preferentially heating either the edge of the plasma or the core at constant density. This will be accomplished by choosing sources with different tangency radii. The temporal

evolution of these edge-heated discharges may also enable us to examine whether an inward heat pinch is present. An inward heat pinch would affect the conventional thermal diffusion analysis which was used to analyze the pellet-fueled discharges. Direct edge heating can also be used to test the hypothesis proposed by Rebut and Hugon (1985) about local heating versus power radiated in determining the stability of magnetic islands.

VII. Major-Radius Compression Experiments

Compression experiments in which the plasma major radius was reduced from 3.0 to 2.1 m in ~ 20 ms have been performed in TFTR. In an initial series of experiments, Tait et al. (1985) observed that the increase in $T_e(0)$ was less than theoretically expected, though the discrepancy in $n_e(0)$ scaling was less. Furthe experiments and analysis (Kiraly et al. 1985) indicate that high frequency MHD activity during compression as well as the occurrence of an exceptionally large internal disruption [sawtooth oscillation] may be important to the understanding and interpretation of these results. Additional experiments are planned to clarify the role of MHD activity and to evaluate transport during compression. During the two neutral beam run period, acceleration of beam ions was studied in 450 kA discharges that were compressed from 3.0 m to 2.17 m in ~ 15 ms. The tangentially coinjected deuterium beam ions were accelerated from 82 to 150 keV in good agreement with Fokker-Planck simulations as shown in Fig. 8 (Wong et al. 1985, and Kaita et al. 1986). Measurements of the neutron emission from $d(d,n)^3He$ reactions and of 15 MeV protons from $^3He(d, p)\alpha$ reactions show a substantial enhancement of the plasma reactivity as expected. Future effort on plasma compression will focus on utilizing it as a tool to understand plasma transport during the intense auxiliary heating which occurs during compression.

VIII. Energetic Ion Mode

Operation of TFTR at low I_p (0.4-1.0 MA) and high beam power has allowed access to a very-low-density regime ($\bar{n}_e \sim 1 \times 10^{19}$ m^{-3}) characterized by high values of ion temperature and toroidal rotation velocity. In this regime, the density rise saturates during injection and the overall density increase is much less than the integrated number of beam ions injected into the torus. The reduced density rise together with the lower initial density is required for operation in this regime. The dependence of the uncorrected ion temperature measurements (from TiXXI K_α Doppler broadening and near-perpendicular passive hydrogen charge-exchange analysis) on absorbed beam power normalized by line-averaged density is shown in Fig. 9. Substantial corrections to both ion temperature measurements are calculated. The impurity ion temperatures need to be corrected for the preferential coupling of the beam power to the impurity ions (Eubank et al. 1979). In addition, smaller corrections due to the emission profile and the shear in the toroidal velocity affect these measurements. The charge-exchange measurements are corrected for emission profile, plasma opacity, and the high toroidal velocity. Central hydrogen temperatures up to 9 ± 2 keV have been achieved. The ion-heating efficiency, $\eta_i = \Delta T_i \bar{n}_e / P_{abs}$, in this regime is similar to that in the standard regime (Medley et al. 1985).

The central toroidal velocity is measured by the Doppler shift of the TiXXI K_α line and increases linearly with $P_{inj}/\bar{n}_e$ up to 7 x 10^5 m/s as shown in Fig. 10. This corresponds to a ratio of $V_\phi(0)/v_H \equiv V_\phi(0)/(T_i/m_H)^{1/2} \simeq 0.6$. At modest values of the parameter $P_{inj}/\bar{n}_e$, measurements of the toroidal velocity using the m = 1 sawtooth precursor are in good agreement with the Ti K_α line Doppler shift measurements. At high power, sawteeth and the m = 1 precursor are not observed.

During neutral beam injection, the surface voltage decreases substantially. Experiments utilizing three co-beamlines have resulted in negative surface voltages ($V_s \simeq -0.15$ V) with P_{inj} of ~ 8 MW in a 700 kA discharge with $\bar{n}_e = 2 \times 10^{19}$ m^{-3}. The surface voltage at the end of the injection pulse decreases with increasing power and increases with increasing current. TRANSP analysis and BALDUR simulations, which do not yet include the effects of plasma rotation, predict a neutral-beam-driven current of 300-500 kA with $P_{inj} \sim 5$ MW. A more quantitative comparison between theory and experiment requires the inclusion of plasma rotation in the time-dependent analysis. The usual assumption that the plasma motion is negligible compared with the fast-ion velocity is not adequate in this regime, substantially complicating the analysis of these discharges (Goldston 1985). Inclusion of these effects in the time-independent code, SNAP, results in a significant reduction in the beam density, a reduction in direct beam heating, and the addition of viscous heating. Further work on evaluating the effects of rotation is in progress. Despite a large population of beam ions and high toroidal velocity, the behavior of the ion heating, momentum confinement, and global energy confinement is similar to that observed in the standard neutral-beam-heating regime. With the addition of a beamline oriented in the counter-direction, the effects of plasma rotation and beam current drive on confinement will be readily studied. Furthermore, in this configuration, substantial enhancements in neutron production from collisions between co- and counter-streaming fast ions are expected, especially if tritium and deuterium beams are used simultaneously.

IX. Conclusions

The difficult problems associated with making high-field, high-current, high-electron density, and high-purity discharges have been successfully resolved in TFTR. Ohmic discharges spanning a wide range of operating parameters provide a variety of interesting target plasmas for neutral beam injection. Pellet injection can create target plasmas with exceptionally high central densities and long energy confinement times. The initial neutral-beam-heating experiments with two beamlines have further expanded the operating parameters. During the next phase of operation, the emphasis will be to gain a better understanding of the transport properties in order to optimize the energy confinement time. Techniques for the enhancement of τ_E that would be effective at high power in a large undiverted tokamak could have a significant impact on the design of future DT reactors. Experiments in the low-density energetic ion regime offer an alternative approach to achieving $Q \sim 1$ and are of basic physics interest. The acceleration of beam ions during compression has been demonstrated to increase the plasma reactivity as expected. The four large tokamaks - JET, JT-60, and TFTR, which are now in operation, and T-15 which is under construction - have been optimized differently. Their roles in the advancement of fusion research are quite distinctive and each device will be able to make a unique contribution.

Acknowledgements

We are grateful to D.J. Grove, H.P. Furth, P.H. Rutherford, and J.R. Thompson for their advice and support and to J. Strachan and W. Heidbrink for useful discussions. This work was supported by US DOE Contract No. DE-AC02-76CH03073. The ORNL participants were also supported by US DOE Contract No. DE-AC05-84OR21400 with Martin Marietta Energy Systems, Inc.

References

Alikaev, V.V. et al. 1985 In Plasma Physics and Controlled Nuclear Fusion Research I IAEA, Vienna, 419-432.

Ashby, D.E.T.F. and Hughes M.H. 1981 Nucl. Fusion 21, 911-926.

Budny, R. et al. 1984 J. Nucl. Mater. 121, 294-303.

Combs, S.K. et al. 1985 Rev. Sci. Instrum. 56, 1173-1178.

Coppi, B. 1980 Comments Plasma Phys. Cont. Fusion 5, 261-269.

Dylla, H.F. 1986 Princeton Plasma Physics Laboratory Report # 2307 (to be published in J. Vac. Sci. and Technol).

Efthimion, P.C. et al. 1984 Phys. Rev. Lett. 52, 1492-1495.

Efthimion, P.C. et al. 1985 In Plasma Physics and Controlled Nuclear Fusion Research I IAEA, Vienna, 29-44.

Eubank, H.P. et al. 1979 In Plasma Physics and Controlled Nuclear Fusion Research I IAEA, Vienna, 167-198.

Eubank, H.P. et al. 1985 In Plasma Physics and Controlled Nuclear Fusion Research I IAEA, Vienna, 303-318.

Fonck, R.J. et al. 1984 In Proceedings of the 4th International Symposium on Heating in Toroidal Plasmas, Rome, 1984 (ENEA, Frascatti, 1984) I, pp. 37-56.

Furth, H.P. et al. 1985 In Proceedings of the 12th European Conference on Controlled Fusion and Plasma Physics (Budapest, Hungary), Contr. papers II, pp. 358-365.

Furth, H.P. 1985 Workshop on Basic Physical Processes of Toroidal Fusion Plasmas (Varenna, Italy), August 26-31, 1985 (to be published).

Gibson, A. 1976 Nucl. Fusion 16, 546-550.

Goldston, R.J. et al. 1981 J. Comput. Phys. 43, 61-78.

Goldston, R.J. 1984 Plasma Phys. and Control Fusion 26, 87-99.

Goldston, R.J. 1985 Workshop on Basic Physical Processes of Toroidal Fusion Plasmas (Varenna, Italy) August 26-31, 1985 (to be published).

Greenwald, M. et al. 1985 In Plasma Physics and Controlled Nuclear Fusion Research London, September 12-19, 1984 (IAEA, Vienna, 1985) Vol. 1, pp. 45-55.

Hawryluk, R.J. 1980 In Proceedings of the Course in Physics Close to Thermonuclear Conditions (Varenna, Italy), Report EUR-FU-BRU/XII/476/80, pp. 503-531.

Hawryluk, R.J. et al. 1984 In Proceedings of the 4th International Symposium on On Heating in Toroidal Plasmas, Rome (Inter. School of Plasma Physics, Varenna) pp. 1012-1032.

Hendel, H.W. (1986), IEEE Transactions on Nucl. Sci. 33, 670-674.

Jassby, D.L. 1977 Nucl. Fusion 17, 309-363.

Johnson, L.C. and Young, K.M. 1983 In Proceedings of the Course on Diagnostics for Fusion Reactor Conditions (1982, Varenna, Italy) held in Varenna (Como), Italy, September 6-17, 1982. New York: Pergamon Press, 1983 2, pp. 551-571.

Kaita, R. et al. 1986 Princeton Plasma Physics Laboratory Report # 2321, submitted to Nucl. Fusion.

Karzas, W.J. and Latter, R. 1961 Astrophys. J. Suppl. Series 6, 167-212.

Kaye, S.M. 1985 Phys. Fluids 28, 2327-2343.

Kaye, S.M. et al. 1984 Nucl. Fusion 24, 1303-1334.

Keilhacker, M. et al. 1985 In Plasma Physics and Controlled Nuclear Fusion Research London, September 12-19, 1984 (IAEA, Vienna, 1985) Vol 1, pp. 71-85.

Kiraly, J. et al. 1985 Princeton Plasma Physics Laboratory Report # 2254.

Kitsunezaki, A. et al. 1985 In Plasma Physics and Controlled Nuclear Fusion Research London, September 12-19, 1984 (IAEA, Vienna, 1985) Vol. 1, pp. 57-65.

Lazarus, E.A. et al. 1984 J. Nucl. Mater. 121, 61-68.

Lipschultz, B. et al. 1984 Nucl. Fusion 24, 977-988.

Medley, S.S. et al. 1985 In Proceedings of the 12th European Conference on Controlled Fusion and Plasma Physics (Budapest, Hungary) Contributed paper I, pp. 343-346.

McGuire, K. et al. 1985 In Proceedings of the 12th European Conference on Controlled Fusion and Plasma Physics (Budapest, Hungary) Contributed paper I, 134-137

Mueller, D. et al. 1986 Discharge Control and Evolution in TFTR. In Proceedings of the 7th Course of the International School of Fusion Reactor Technology (Erice, Italy, July 1985), pp. 143-157. New York: Plenum Publishing Corporation.

Murakami, M. et al. 1985a In Proceedings of the 6th Topical Meeting on the Technology of Fusion Energy (San Francisco, March 1985), Fusion Technology 8, part 2A, 657-663.

Murakami, M. et al. 1985b In Proceedings of the 12th European Conference on Controlled Fusion and Plasma Physics (Budapest, Hungary) Invited paper to be published.

Ohyabu, N. 1979 Nucl. Fusion 19, 1491-1497.

Overskei, D. et al. 1984 In Proceedings of the 4th International Symposium on Heating in Toroidal Plasmas, Rome, 1984 (ENEA, Frascatti, 1984) I, Vol. 1, pp. 21-36.

Pease, R.S. 1957 Proc. of the Phys. Soc. B, LXX, 11-23.

Perkins, F.W. 1984 In Proceedings of the 4th International Symposium on Heating in Toroidal Plasmas, Rome (Int. School of Plasma Physics, Varenna) pp. 977-988.

Perkins, F.W. and Hulse, R.A. 1985 Phys. of Fluids 28, 1837-1844.

Rebut, P.H. and Greene, B.J. 1977 In Plasma Physics and Controlled Nuclear Fusion Research, 1976 (IAEA, Vienna) Vol. 2, pp. 3-16.

Rebut, P.H. and Hugon, M. 1985 In Plasma Physics and Controlled Nuclear Fusion Research II IAEA, Vienna, 197-212.

Roberts, D.E. 1983 Nucl. Fusion 23, 311-329.

Schmidt, G.L. et al. 1985 In Proceedings of the 12th European Conference on Controlled Fusion and Plasma Physics (Budapest, Hungary), Contr. papers II, pp. 674-677.

Sengoku, S. et al. 1985 In Plasma Physics and Controlled Nuclear Fusion Research London, September 12-19, 1984 (IAEA, Vienna, 1985) Vol. 1, pp. 405-415.

Speth, E. et al. 1985 In Proceedings of the 12th European Conference on Controlled Fusion and Plasma Physics (Budapest, Hungary), Contr. Papers II, pp. 284-287.

Strachan, J.D. et al. 1985 In Proceedings of the 12th European Conference on Controlled Fusion and Plasma Physics (Budapest, Hungary), Contr. Papers I, pp. 339-342.

Tait, G. et al. 1985 In Plasma Physics and Controlled Nuclear Fusion Research London, September 12-19, 1984 (IAEA, Vienna, 1985) Vol. I, pp. 141-154.

Taylor, G. et al. 1985 Princeton Plasma Physics Laboratory Report #2221. (August 1985); 1986 Nucl. Fusion 26 No. 3, 339-348.

Wong, K.L. et al. 1985 Phys. Rev. Lett. 55, 2587-2590.

Zweben, S.J., Redi, M.H. and Bateman, G. 1986 Princeton Plasma Physics Laboratory Report # 2316.

Table 1

Neutral Beam System Parameters

	April 1985	February 1986	April 1987
Pulse Length (sec)	0.5	0.5	2.0
Voltage (kV)	80	80	120
Number of Beamlines	2	4	4
Ion Sources	6	11	12
Beamline Configuration	2-co	3-co 1-ctr	3-co 1-ctr
Power (MW) (deuterium)	6.3	11	27
Power at Full Energy	3	5.5	20

Figure Captions

Figure 1 Operating range of TFTR gas-fueled and pellet-fueled deuterium discharges conducted on the moveable limiter. q_a is the limiter safety factor.

Figure 2 Gross energy confinement versus $\bar{n}_e q R^2 a$ for ohmically heated discharges with and without pellet injection. These experiments were performed on the moveable limiter in the large plasma configuration.

Figure 3 Variation of the electron, ion, and beam-stored energy with heating power for the 2.2 MA power scan. Diamagnetic measurements of stored energy are shown for comparison.

Figure 4 Variation of the gross energy confinement time for the power scan and comparison with L- and H-mode scaling model of Goldston (1984).

Figure 5 Dependence of the gross energy confinement on plasma current for experiments conducted on the moveable limiter during experiments performed with two neutral beamlines.

Figure 6 Ratio of volume-averaged electron temperature to central electron temperature as a function of the inverse of the limiter safety factor. All data points are averaged over several sawtooth periods, except the data shown by a vertical line which is bounded by two values for the $T_e(r)$ profiles before and after a large internal disruption (sawtooth oscillation).

Figure 7 Fractional total stored energy within r = a/3 versus fractional heating power deposited within r = a/3. The shaded area indicates a large number (~200) of ohmically heated discharges.

Figure 8 Charge-exchange measurements of the fast-ion slowing-down spectra before and after major-radius compression commencing at 2.5 sec. The dashed curves are Fokker-Planck simulations.

Figure 9 Dependence of the uncorrected ion temperature measurements based on Doppler broadening of T_i K_α lines (T_{imp}) and perpendicular charge-exchange spectra [$T_i(cx)$] as a function of $P_{inj}/\bar{n}_e$. The correction to the measurements is shown by the arrows.

Figure 10 Central toroidal rotation velocity as a function of the ratio of injected beam power to line-averaged electron density.

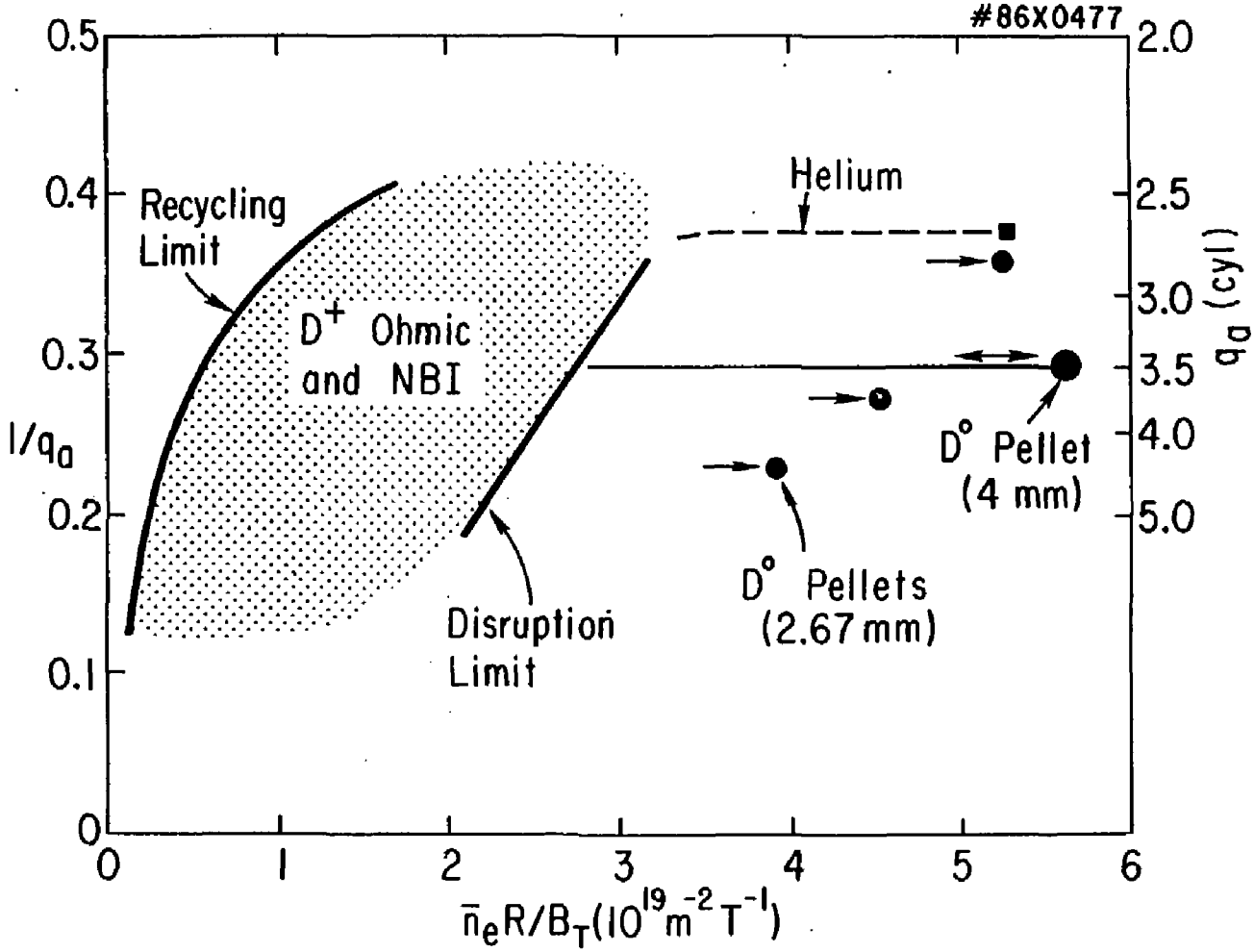
#86X0477
0.5
0.4
0.3
0.2
0.1
0
$1/q_a$
2.0
2.5
3.0
3.5
4.0
5.0
q_a (cyl)
Recycling Limit
D^+ Ohmic and NBI
Helium
D° Pellet (4 mm)
D° Pellets (2.67 mm)
Disruption Limit
0
1
2
3
4
5
6
$\bar{n}_e R/B_T (10^{19} m^{-2} T^{-1})$

Fig. 1

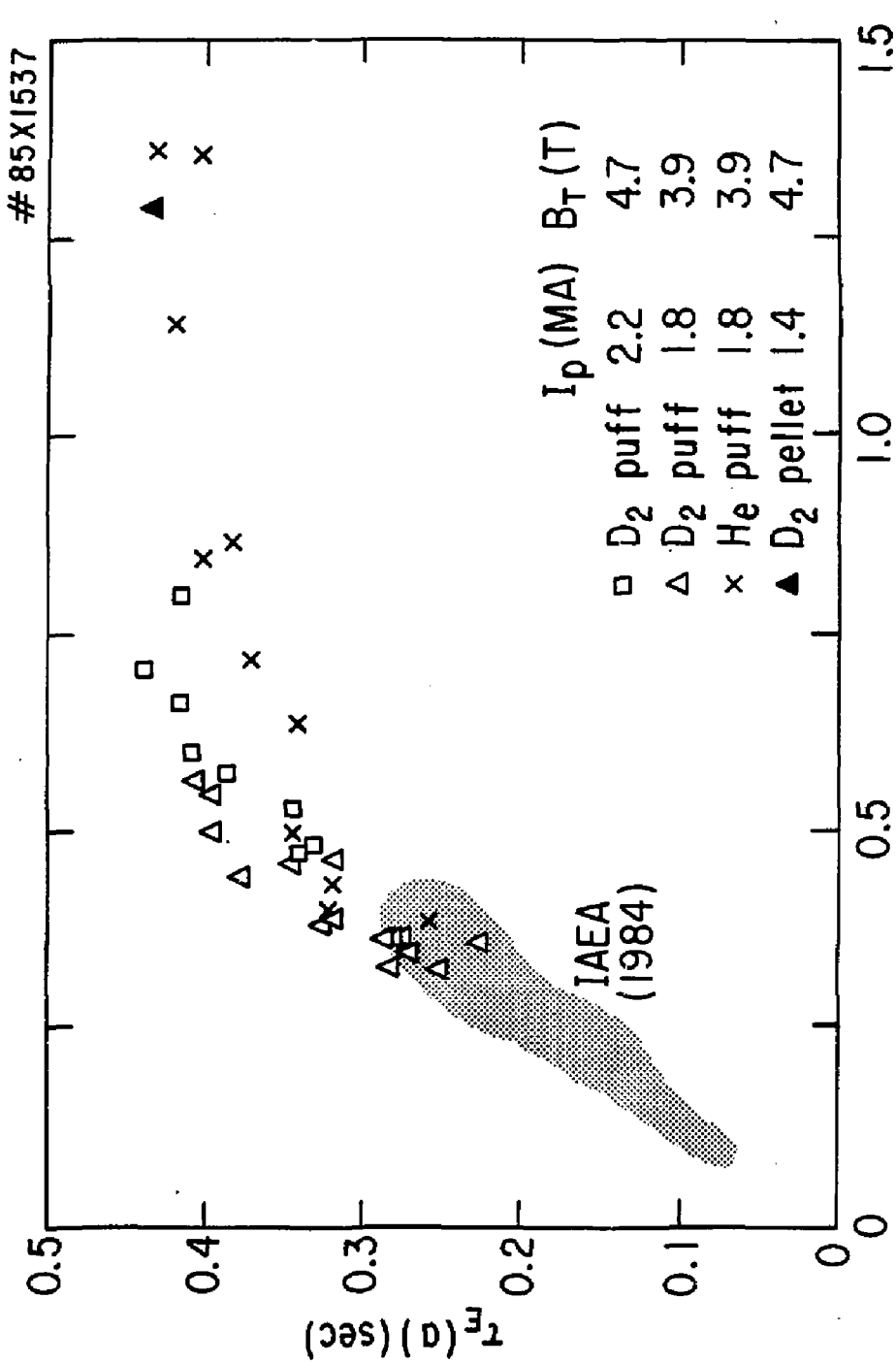
#85X1537
τ_E(Q) (sec)
$\bar{n}_e q R^2 a$ (10^{21})
I_p (MA) B_T (T)
□ D_2 puff 2.2 4.7
△ D_2 puff 1.8 3.9
× He puff 1.8 3.9
▲ D_2 pellet 1.4 4.7
IAEA (1984)
0
0.1
0.2
0.3
0.4
0.5
0.5
1.0
1.5

Fig. 2

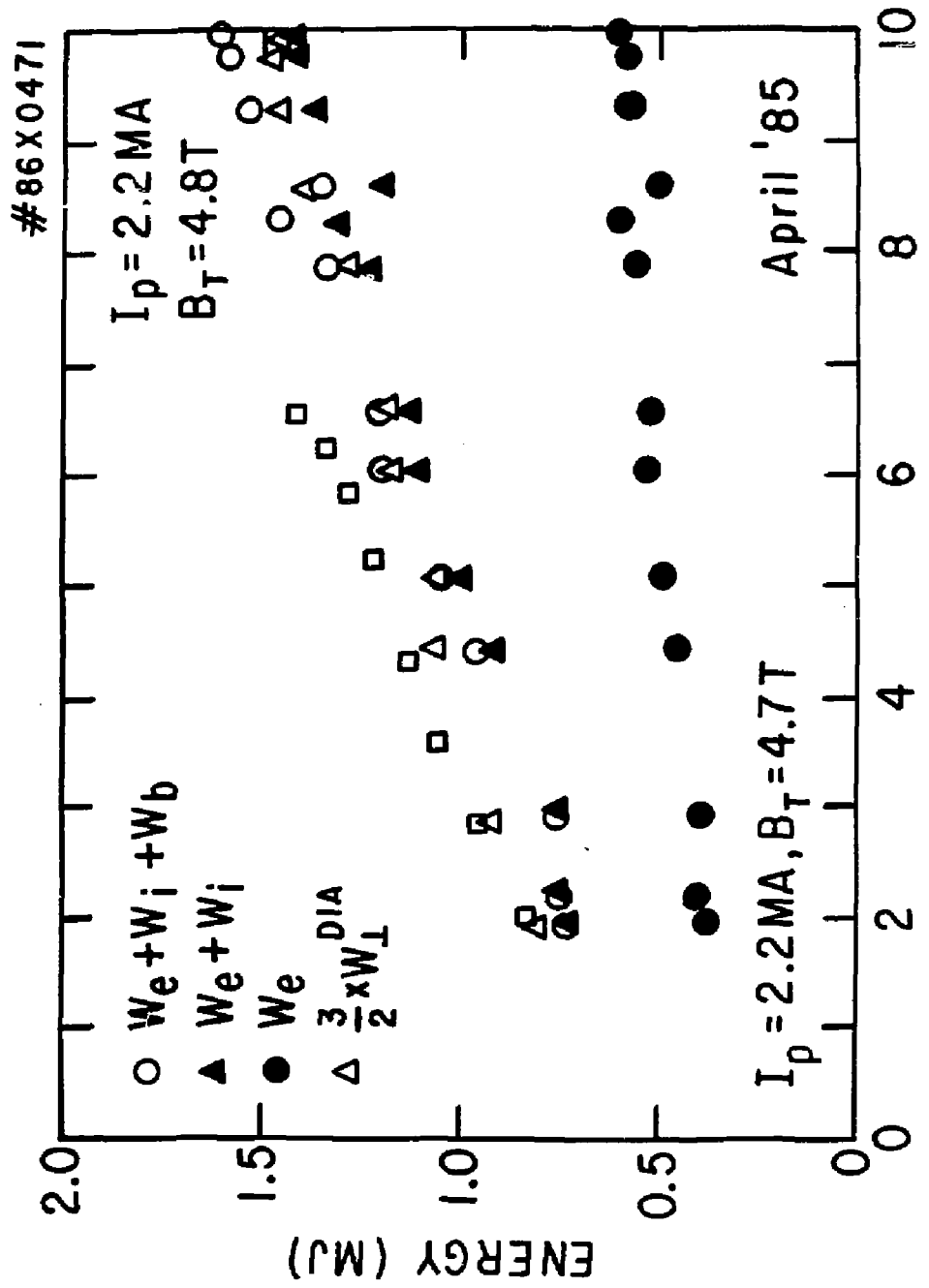
#86X0471
I_p= 2.2 MA
B_T=4.8T
April '85
I_p=2.2MA, B_T=4.7T
$W_e+W_i+W_b$
W_e+W_i
W_e
$\frac{3}{2}xW_\perp^{DIA}$
ENERGY (MJ)
P_{heat} (MW)
0
0.5
1.0
1.5
2.0
2
4
6
8
10

Fig. 3

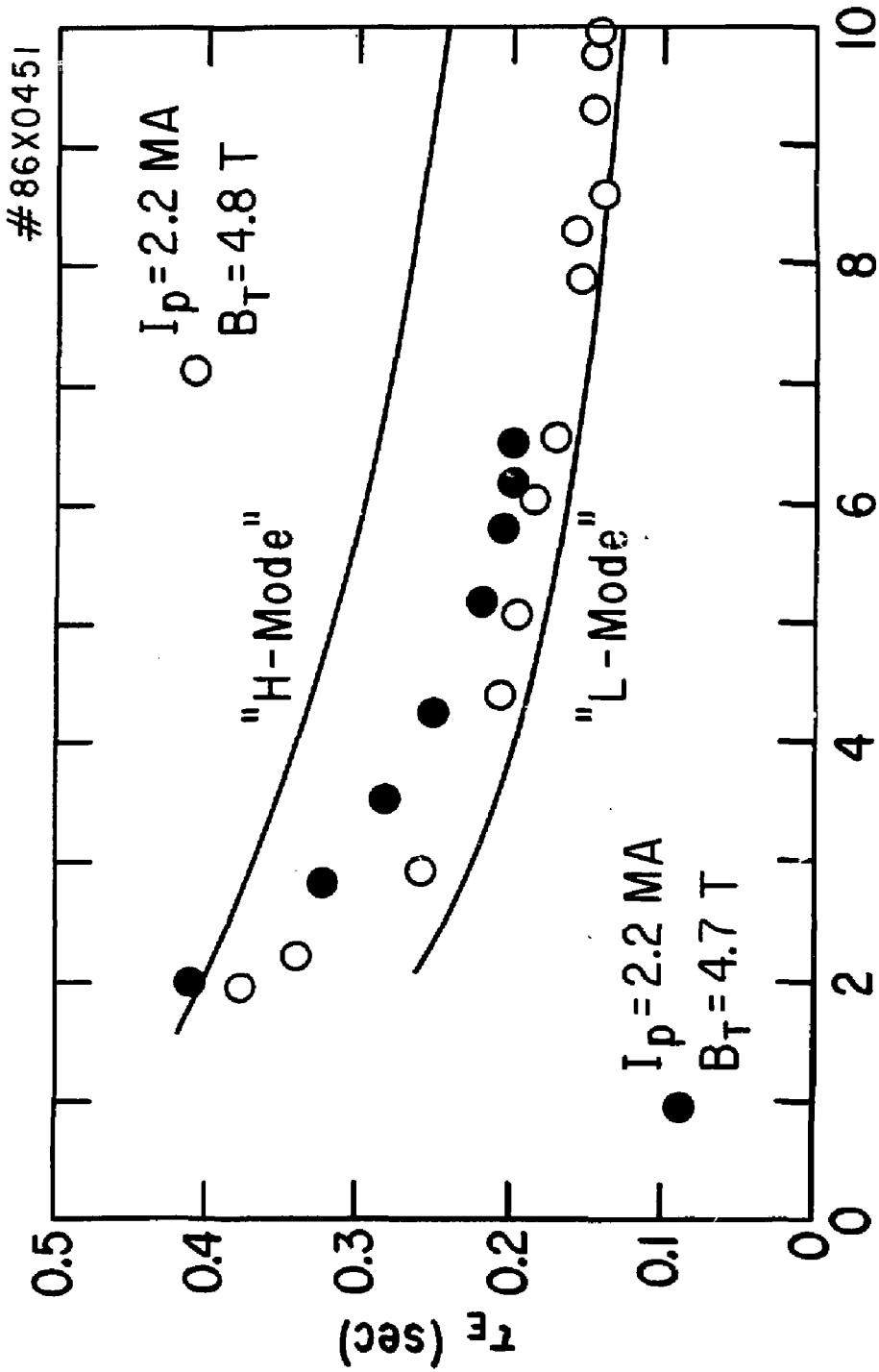
#86X0451
I_p=2.2 MA
B_T=4.8 T
"H-Mode"
"L-Mode"
I_p=2.2 MA
B_T=4.7 T
τ_E (sec)
P_{heat} (MW)
0.5
0.4
0.3
0.2
0.1
0
0
2
4
6
8
10

Fig. 4

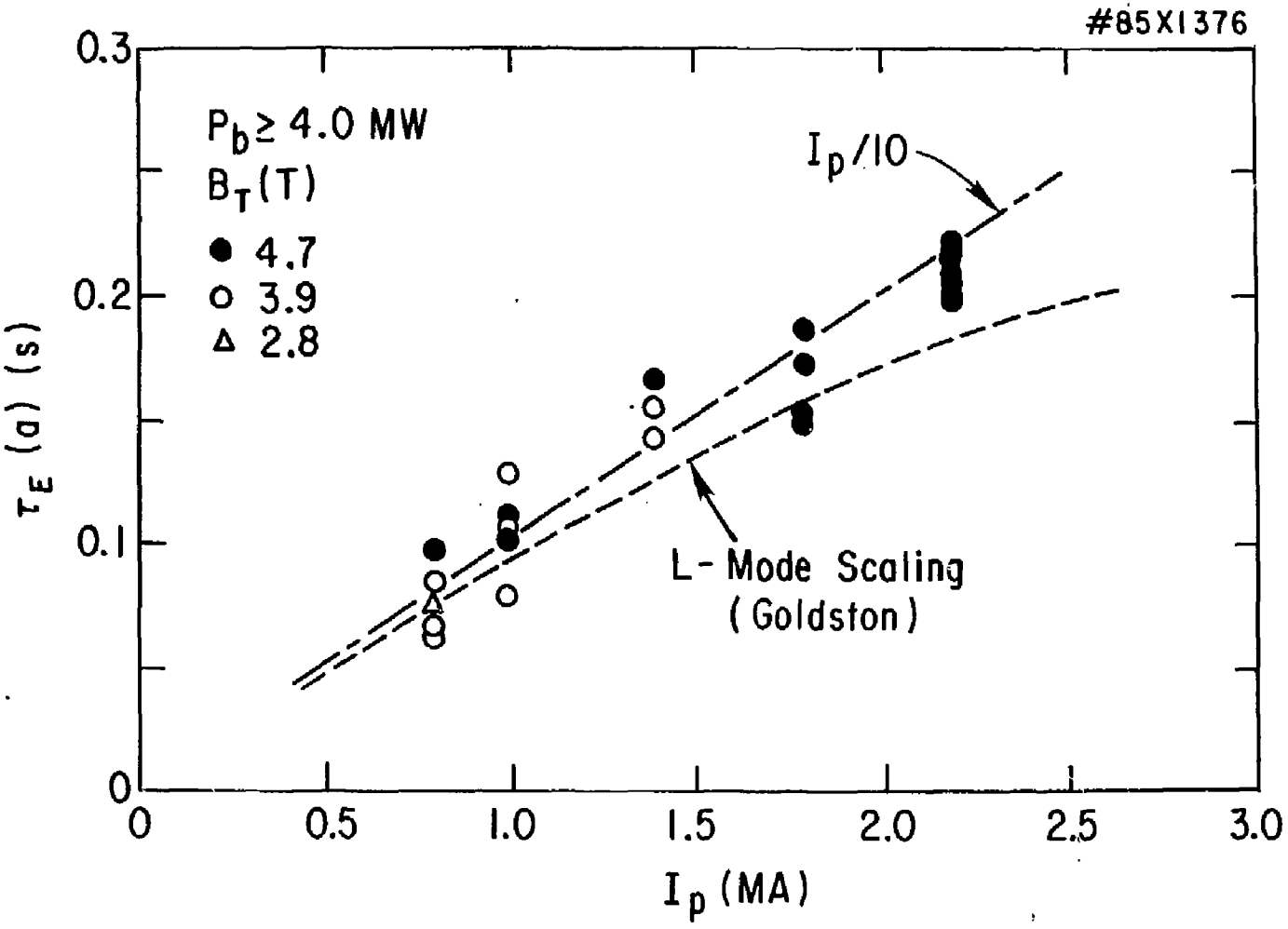
#85X1376
$P_b \geq 4.0$ MW
B_T(T)
● 4.7
○ 3.9
△ 2.8
$I_p/10$
L-Mode Scaling
(Goldston)
τ_E (a) (s)
I_p (MA)
0.3
0.2
0.1
0
0
0.5
1.0
1.5
2.0
2.5
3.0

Fig. 5

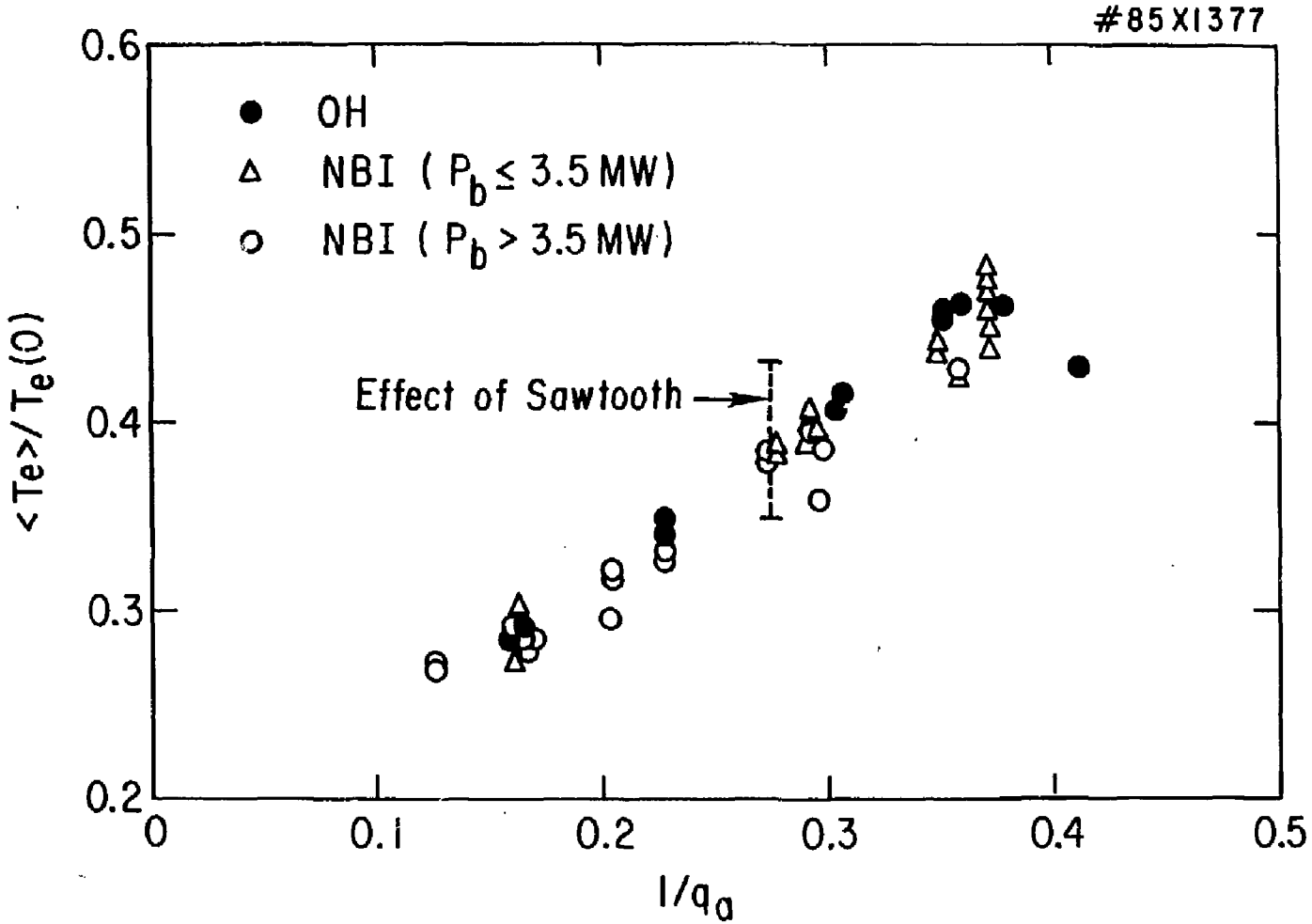
#85X1377
OH
NBI ($P_b \leq 3.5$ MW)
NBI ($P_b > 3.5$ MW)
Effect of Sawtooth
$<Te>/T_e(0)$
$1/q_a$
0.6
0.5
0.4
0.3
0.2
0
0.1
0.2
0.3
0.4
0.5

Fig. 6

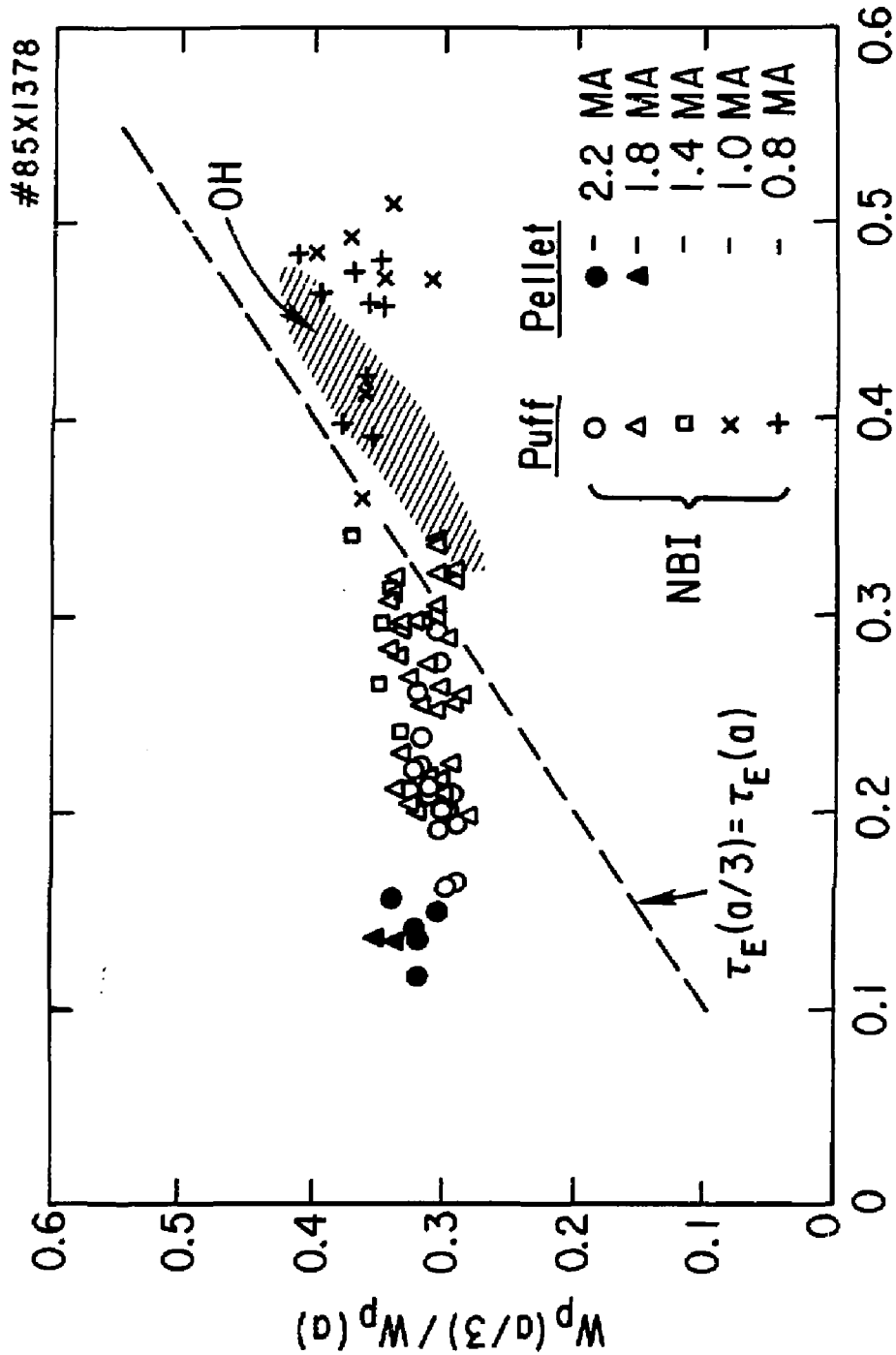
#85X1378
OH
Puff
Pellet
NBI
2.2 MA
1.8 MA
1.4 MA
1.0 MA
0.8 MA
$\tau_E(a/3) = \tau_E(a)$
$W_p(a/3) / W_p(a)$
$P_{heat}(a/3) / P_{heat}(a)$
0
0.1
0.2
0.3
0.4
0.5
0.6

Fig. 7

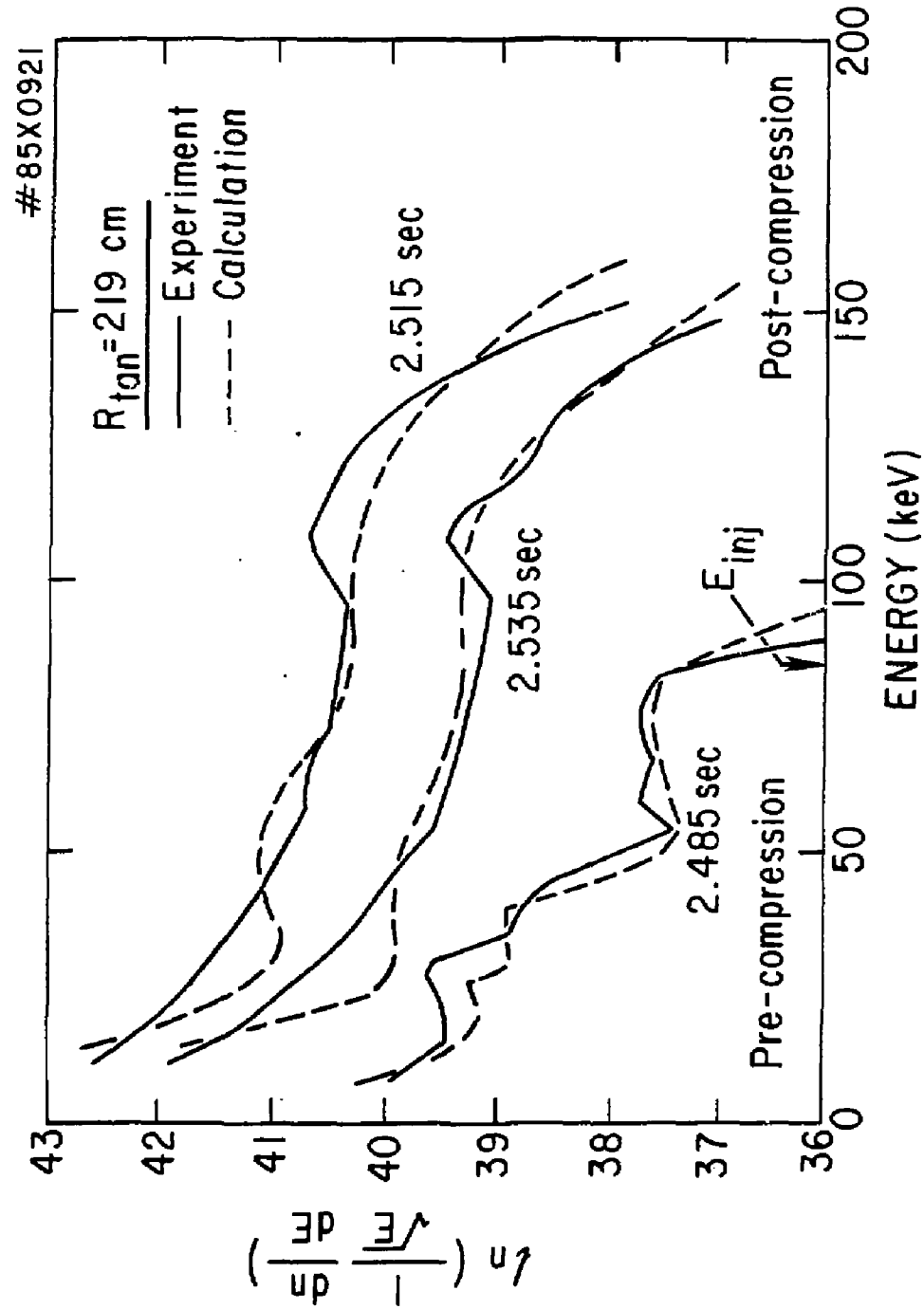
#85X0921
R_{tan}=219 cm
Experiment
Calculation
2.515 sec
2.535 sec
2.485 sec
E_{inj}
Pre-compression
Post-compression
ENERGY (keV)
$\ln\left(\frac{1}{\sqrt{E}}\frac{dn}{dE}\right)$
43
42
41
40
39
38
37
36
0
50
100
150
200

Fig. 8

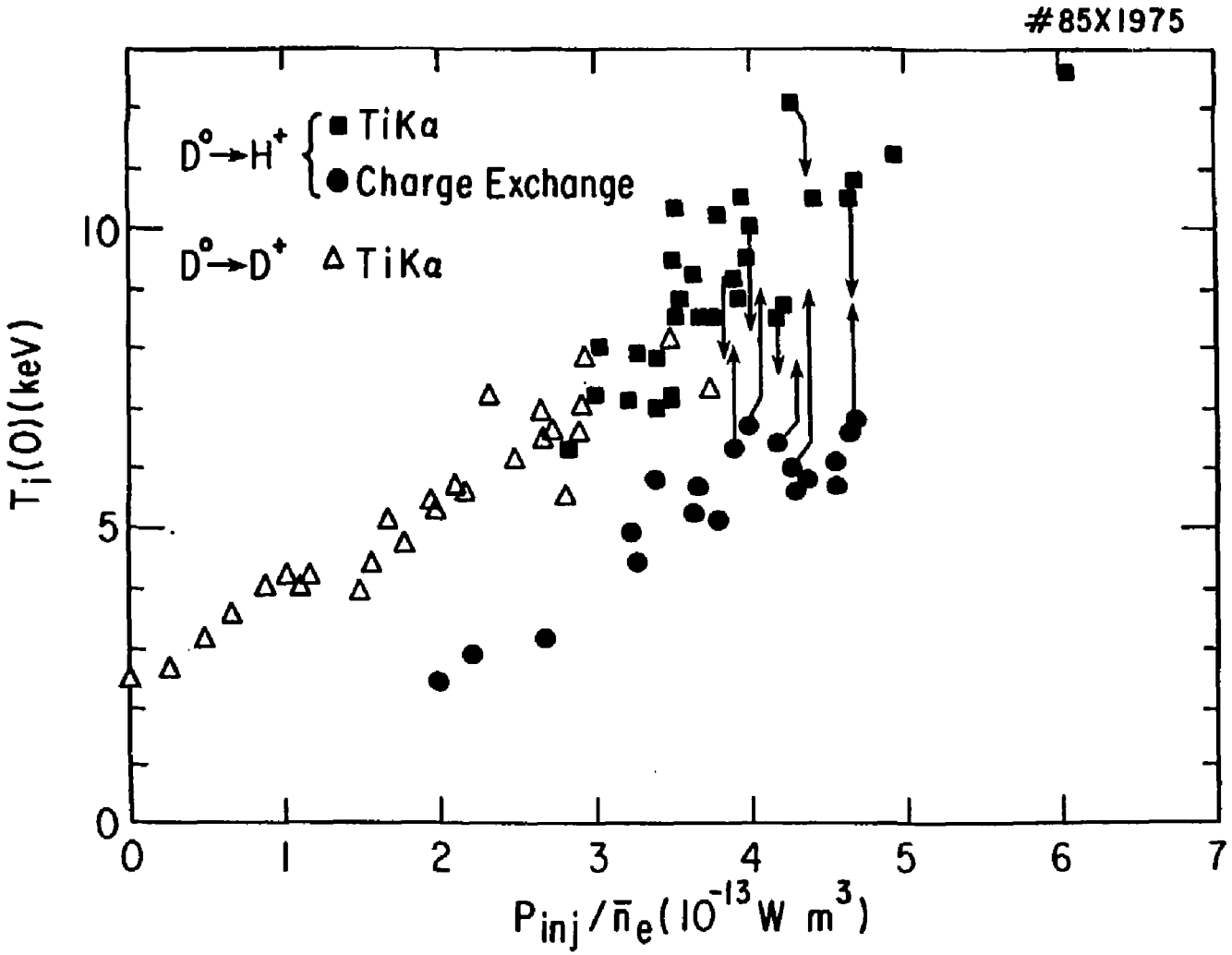
#85X1975
D°→H⁺ { ■ TiKα
● Charge Exchange
D°→D⁺ △ TiKα
$T_i(0)$(keV)
$P_{inj}/\bar{n}_e(10^{-13}$W m$^3)$
0
5
10
0
1
2
3
4
5
6
7

Fig. 9

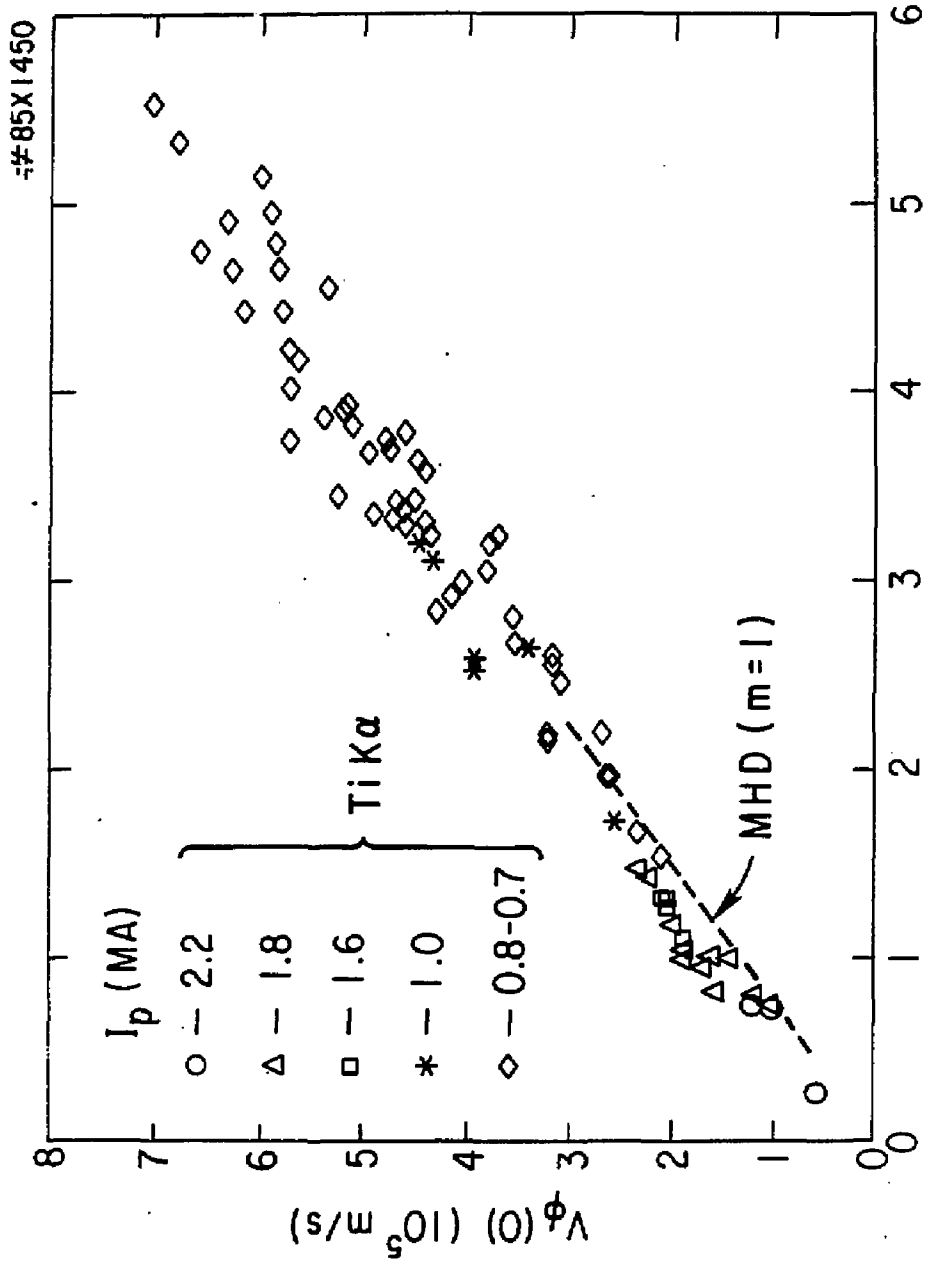
#85X1450
$V_\phi(0)$ (10^5 m/s)
$P_{inj}/\bar{n}_e$ (10^{-13} w·m^3)
I_p (MA)
○ – 2.2
△ – 1.8
□ – 1.6
* – 1.0
◇ – 0.8-0.7
Ti Kα
MHD (m=1)

Fig. 10

EXTERNAL DISTRIBUTION IN ADDITION TO UC-20

Plasma Res Lab, Austra Nat'l Univ, AUSTRALIA
Dr. Frank J. Paoloni, Univ of Wollongong, AUSTRALIA
Prof. I.R. Jones, Flinders Univ., AUSTRALIA
Prof. M.H. Brennan, Univ Sydney, AUSTRALIA
Prof. F. Cap, Inst Theo Phys, AUSTRIA
M. Goossens, Astronomisch Instituut, BELGIUM
Prof. R. Boucique, Laboratorium voor Natuurkunde, BELGIUM
Dr. D. Palumbo, Dg XII Fusion Prog, BELGIUM
Ecole Royale Militaire, Lab de Phys Plasmas, BELGIUM
Dr. P.H. Sakanaka, Univ Estadual, BRAZIL
Lib. & Doc. Div., Instituto de Pesquisas Espaciais, BRAZIL
Dr. C.R. James, Univ of Alberta, CANADA
Prof. J. Teichmann, Univ of Montreal, CANADA
Dr. H.M. Skarsgard, Univ of Saskatchewan, CANADA
Prof. S.R. Sreenivasan, University of Calgary, CANADA
Prof. Tudor W. Johnston, INRS-Energie, CANADA
Dr. Hannes Barnard, Univ British Columbia, CANADA
Dr. M.P. Bachynski, MPB Technologies, Inc., CANADA
Chalk River, Nucl Lab, CANADA
Zhengwu Li, SW Inst Physics, CHINA
Library, Tsing Hua University, CHINA
Librarian, Institute of Physics, CHINA
Inst Plasma Phys, Academia Sinica, CHINA
Dr. Peter Lukac, Komenskeho Univ, CZECHOSLOVAKIA
The Librarian, Culham Laboratory, ENGLAND
Prof. Schatzman, Observatoire de Nice, FRANCE
J. Radet, CEN-BP6, FRANCE
JET Reading Room, JET Joint Undertaking, ENGLAND
AM Dupas Library, AM Dupas Library, FRANCE
Dr. Tom Mual, Academy Bibliographic, HONG KONG
Preprint Library, Cent Res Inst Phys, HUNGARY
Dr. R.K. Chhajlani, Vikram Univ, INDIA
Dr. B. Dasgupta, Saha Inst, INDIA
Dr. P. Kaw, Physical Research Lab, INDIA
Dr. Phillip Rosenau, Israel Inst Tech, ISRAEL
Prof. S. Cuperman, Tel Aviv University, ISRAEL
Prof. G. Rostagni, Univ Di Padova, ITALY
Librarian, Int'l Ctr Theo Phys, ITALY
Miss Clelia De Palo, Assoc EURATOM-ENEA, ITALY
Biblioteca, del CNR EURATOM, ITALY
Dr. H. Yamato, Toshiba Res & Dev, JAPAN
Direc. Dept. Lg. Tokamak Dev. JAERI, JAPAN
Prof. Nobuyuki Inoue, University of Tokyo, JAPAN
Research Info Center, Nagoya University, JAPAN
Prof. Kyoji Nishikawa, Univ of Hiroshima, JAPAN
Prof. Sigeru Mori, JAERI, JAPAN
Prof. S. Tanaka, Kyoto University, JAPAN
Library, Kyoto University, JAPAN
Prof. Ichiro Kawakami, Nihon Univ, JAPAN
Prof. Satoshi Itoh, Kyushu University, JAPAN
Dr. D.I. Choi, Adv. Inst Sci & Tech, KOREA
Tech. Info Division, KAERI, KOREA
Bibliotheek, Fom-Inst Voor Plasma, NETHERLANDS
Prof. B.S. Liley, University of Waikato, NEW ZEALAND
Prof. J.A.C. Cabral, Inst Superior Tecn, PORTUGAL
Dr. Octavian Petrus, ALI CUZA University, ROMANIA
Prof. M.A. Hellberg, University of Natal, SO AFRICA
Dr. Johan de Villiers, Plasma Physics, Nucor, SO AFRICA
Fusion Div. Library, JEN, SPAIN
Prof. Hans Wilhelmson, Chalmers Univ Tech, SWEDEN
Dr. Lennart Stenflo, University of UMEA, SWEDEN
Library, Royal Inst Tech, SWEDEN
Centre de Rechercheson, Ecole Polytech Fed, SWITZERLAND
Dr. V.T. Tolok, Kharkov Phys Tech Ins, USSR
Dr. D.D. Ryutov, Siberian Acad Sci, USSR
Dr. G.A. Eliseev, Kurchatov Institute, USSR
Dr. V.A. Glukhik.., Inst Electro-Physical, USSR
Institute Gen. Physics, USSR
Prof. T.J.M. Boyd, Univ College N Wales, WALES
Dr. K. Schindler, Ruhr Universitat, W. GERMANY
ASDEX Reading Rm, IPP/Max-Planck-Institut fur Plasmaphysik, F.R.G.
Nuclear Res Estab, Julich Ltd, W. GERMANY
Librarian, Max-Planck Institut, W. GERMANY
Bibliothek, Inst Plasmaforschung, W. GERMANY
Prof. R.K. Janev, Inst Phys, YUGOSLAVIA